Available online at www.sciencedirect.com
ScienceDirect
International Journal of Multiphase Flow 32 (2006) 1326–1339
International Journal of Multiphase Flow
www.elsevier.com/locate/ijmulflow

On the influence of near-wall forces in particle-laden channel flows

B. Arcen, A. Tanière *, B. Oesterlé

LEMTA – UMR 7563 CNRS, ESSTIN, Université Henri Poincaré-Nancy 1, 2 rue Jean Lamour, F-54529 Vandoeuvre-lès-Nancy, France

Received 16 February 2006; received in revised form 16 June 2006

Abstract

Computation of a turbulent dilute gas–solid channel flow has been undertaken to study the influence of using wall-corrected drag coefficients and of the lift force on the dispersed phase characteristics. The incompressible Navier–Stokes equations governing the carrier flow were solved by using a direct numerical simulation approach and coupled with a Lagrangian particle tracking. Calculations were performed at Reynolds number based on the wall-shear velocity and channel half-width, $Re_\tau \approx 184$, and for three different sets of solid particles. For each particle set, two cases were examined, in the first one the particle motion was governed by both drag and lift wall-corrected forces, whereas in the other one, the standard drag force (not corrected) was solely acting. The lift force model used represents the most accurate available expression since it accounts for weak and strong shear as well as for wall effects. For this study, we considered elastic collisions for particles contacting the walls and that no external forces were acting. Present results indicate that the use of the lift force and of the drag corrections does not lead to significant changes in the statistical properties of the solid phase, at the exception of some statistics for the high inertia particles.

Keywords: DNS; Gas–solid flow; Near-wall effects; Lift; Drag forces

1. Introduction

In order to simulate accurately the dispersion or the deposition phenomena of solid particles in a channel flow, sophisticated numerical techniques, such as direct numerical or large eddy simulation (DNS and LES) coupled with a particle Lagrangian tracking, are often used. Using these numerical approaches requires a choice on the primary forces acting on the particle, and then, on the expressions used for modelling these forces. It can be seen from previous studies of turbulent flows laden with solid particles that the choice of the forces is not universal, especially in wall-bounded flows. Generally, this choice can depend on the phenomena studied. For instance, in particle deposition studies, the lift force is often taken into account (Wang and Squires, 1996a; Wang et al., 1997; Marchioli and Soldati, 2002), and sometimes, in addition the drag force is corrected due to

* Corresponding author. Tel.: +33 383 685 083.
E-mail address: anne.taniere@esstin.uhp-nancy.fr (A. Tanière).

0301-9322/$ - see front matter © 2006 Elsevier Ltd. All rights reserved.
doi:10.1016/j.ijmultiphaseflow.2006.06.009

the presence of the walls (see the work of Chen and McLaughlin (1995)). A possible way to make a choice about the forces is to run simulations in which different forces are accounted for and then to verify which case better reproduces experimental data. For instance, numerous numerical studies have been devoted to the simulation of the experiment by Kulick et al. (1994). Wang and Squires (1996b), using LES under one way coupling assumption and disregarding the drag force correction, tried to simulate the two-phase flow studied by Kulick et al. (1994), however discrepancies between numerical and experimental data were found, especially near the wall. Another attempt is due to Fukagata et al. (1999), who used LES to examine different cases, with one-, two- and four-way coupling effects, using or not drag correction and with two different particle-wall boundary conditions (elastic-bouncing or absorbing walls); however, in their simulation, the lift force was not taken into account. Fukagata et al. (1999) found that the agreement with the experimental data, even under four-way coupling, was still not satisfactory. Recently, Benson et al. (2005) explained the difficulty of earlier numerical simulations to reproduce this experiment by examining the effects of wall roughness on the gas and particle phases in the same vertical channel flow facility as Kulick et al. (1994). They concluded that some of the dispersed phase statistics were a consequence of the poorly defined roughness in the development duct of the channel used by Kulick et al. (1994). The study by Fukagata et al. (1999) has enabled to examine the influence of considering or not the drag correction and of different coupling mechanisms on the dispersed phase statistics, however.

The choice of acceptable assumptions and of the hydrodynamic force models has not yet been clearly stated for the numerical simulations of gas-particles flows. Many questions emerge such as the use of the lift force in the particle dispersion study. And if the lift force is included in the particle equation of motion, which expressions should be used to model it. Wang et al. (1997) introduced a lift force model called "optimum" lift force in order to better predict the dependence of the deposition velocity on particle relaxation time. This optimum lift force takes into account the force due to shear as well as the force due to the presence of the wall. The model is in fact a bundle of different expressions derived in simple flow and is the most appropriated available model of the lift force acting on solid particles in wall-bounded shear flows. Wang et al. (1997) have shown that in deposition study the overall effect of the optimum lift force on their deposition rate results is small. However, as emphasized by them, the small effect on predictions of particle deposition should not be interpreted as the force itself being inaccurate or unimportant.

The objective of the present paper is to discuss the importance of using the lift force and wall-corrections of the drag coefficient for modelling the motion of solid particles in a fully-developed channel flow without external forces. This investigation is conducted by means of direct numerical simulation at moderate Reynolds number. In order to judge the influence of the near-wall corrections, two different cases are examined, in the first one the correction of the drag coefficient and the optimum lift force are taken into account, whereas in the second one, the simulations are conducted without using them. The comparison is made on different kinds of statistics such as the mean drag forces, the mean particle distribution and velocities, the root mean square of the fluid and particles velocities, the drift velocities, and finally the fluid-particle covariance tensor. This comparison is presented for three sets of particles, characterized by different relaxation times.

2. Channel flow DNS and solid particle tracking

The DNS solver, second order accurate in space and in time (Orlandi, 2000), performs the simulation of a turbulent channel flow at $Re_b = 2800$ (based on channel half-width δ and bulk velocity U_b) corresponding to the Reynolds number based on the wall shear velocity equal to 184. The domain size in the streamwise, wall-normal, and spanwise direction is $2.5\pi\delta \times 2\delta \times 1.5\pi\delta$ and the corresponding grid $192 \times 128 \times 160$, respectively. The DNS code was modified to perform Lagrangian tracking of solid particles. The numerical simulation of solid particle trajectories is restricted to spherical particles smaller than the dimension (in wall units) of the smallest cell $\Delta y^+ = 1$ and consequently smaller than the smallest Kolmogorov length scale. Therefore, we made use of the point-force approximation. The solid particle volume fraction is assumed to be relatively small and particle–particle interactions are neglected. In addition, considering that the ratio between the particle and fluid density obeys $\rho_p/\rho_f \gg 1$, the particle equation of motion can be written without taking the added mass, history and spin induced lift forces into account. Under these considerations the equation governing the motion of a solid particle is

$$\frac{\mathrm{d}v_i}{\mathrm{d}t} = \frac{u_i^{\mathrm{p}} - v_i}{\tau_{\mathrm{p}}} + \frac{F_i^{\mathrm{L}}}{m_{\mathrm{p}}}, \tag{1}$$

where F_i^{L} represents the shear-induced lift force, m_{p} is the mass of a single particle, v_i are the particle's velocity components, u_i^{p} are the fluid velocity components interpolated at the solid particle's location defined by $u_i^{\mathrm{p}}(t) = u_i(x_{\mathrm{p},i}(t), t)$. The determination of the interpolated fluid velocity at particle location is therefore crucial. For this purpose a 3D Hermite interpolation based on cubic polynomials is used, this interpolation being a good compromise between accuracy and CPU time expenses (Rovelstad et al., 1994). The aerodynamic forces considered here are the non-linear drag and the shear-induced lift force, both of them are corrected for near-wall effects. The particle relaxation time τ_{p} is expressed in terms of the drag coefficient C_{D} and the magnitude of the relative velocity $\|\mathbf{V}_r\|$ between the particle and the fluid at the particle location.

3. Near-wall force corrections

3.1. Corrected drag force

The drag coefficient C_{D} is computed from the correlation proposed by Morsi and Alexander (1972) since the particle Reynolds number Re_{p} may exceed unity. The particle relaxation time, which obeys $\tau_{\mathrm{p}} = \rho_{\mathrm{p}} d_{\mathrm{p}}^2 / 18\mu$ in the Stokes regime (d_{p} being the particle diameter), is expressed more generally in terms of C_{D} as

$$\tau_{\mathrm{p}} = \frac{4}{3}\frac{\rho_{\mathrm{p}}}{\rho_{\mathrm{f}}}\frac{d_{\mathrm{p}}}{C_{\mathrm{D}}\|\mathbf{V}_r\|}. \tag{2}$$

Close to the wall, the drag is corrected according to the direction of the particle motion, as recommended by Rizk and Elghobashi (1985): the first correction was derived by Faxen (1923) for a particle moving parallel to the wall, and the second one was derived by Maude (1963) for a particle moving normal to the wall. The corresponding correction coefficients are

$$C_{\parallel} = \left(1 - \frac{9}{16}\left(\frac{d_{\mathrm{p}}}{2l}\right) + \frac{1}{8}\left(\frac{d_{\mathrm{p}}}{2l}\right)^3 - \frac{45}{256}\left(\frac{d_{\mathrm{p}}}{2l}\right)^4 - \frac{1}{16}\left(\frac{d_{\mathrm{p}}}{2l}\right)^5\right)^{-1}, \tag{3}$$

$$C_{\perp} = 1 + \frac{9}{8}\left(\frac{d_{\mathrm{p}}}{2l}\right) + \left(\frac{9}{8}\frac{d_{\mathrm{p}}}{2l}\right)^2, \tag{4}$$

where l is defined as the distance between the particle centre and the nearest wall. Such drag corrections are theoretically valid for small values of d_{p}/l, however Rizk and Elghobashi (1985) pointed out that the approximate expression of $C_{\parallel}$ (Eq. 3) is in excellent agreement with the exact analytical results up to $d_{\mathrm{p}}/l = 1.53$. It should be noted that another expression for $C_{\perp}$ has been proposed by Wakiya (1960)

$$C_{\perp} = \left[1 - \frac{9}{8}\left(\frac{d_{\mathrm{p}}}{2l}\right) + \frac{1}{2}\left(\frac{d_{\mathrm{p}}}{2l}\right)^3\right]^{-1}. \tag{5}$$

This expression is correct to $O((d_{\mathrm{p}}/2l)^3)$, whereas the expression from Maude (1963) is an approximation of $C_{\perp}$ correct to $O((d_{\mathrm{p}}/2l)^2)$. One could show, using McLaurin series expansion, that the approximated expression of Wakiya (1960) restricted to $O((d_{\mathrm{p}}/2l)^2)$ is exactly the same as the one proposed by Maude (1963). The exact expression of the drag correction factor, given by infinite series, was established by Brenner (1961) using bipolar coordinate solution of the creeping motion equations. According to Brenner (1961), $C_{\perp} \to \infty$ when $d_{\mathrm{p}}/2l \to 1$, whereas using the expression proposed by Maude (1963) $C_{\perp} \to 3.39$. From the computation of these two expressions, it can be seen that the formula by Maude (1963) underestimates the exact solution from Brenner (1961) when $2l/d_{\mathrm{p}} < 4$. Using Brenner's expression would lead to higher drag correction, and consequently, could increase the residence time of the particles very near the wall. However, this could only occur in a very thin zone and for light particles.

The drag correction coefficients are introduced in the simulations using a corrected particle relaxation time which is simply the particle relaxation time divided by the applied corrections, $\tau_{p\,\mathrm{corrected}}^{\parallel,\perp} = \tau_{\mathrm{p}}/C_{\parallel,\perp}$. According

to Eqs. (3) and (4), the corrected particle relaxation time is found to be smaller in the vicinity of the wall and is dependent on the direction of the particle motion.

3.2. Lift force

The motion of solid particles was computed using the "optimum" lift force as defined by Wang et al. (1997). This force can be divided into two parts, the first one represents the contribution of the velocity shear and the other one represents the presence of the wall. The lift force is only valid within the limit of small particle Reynolds number and in the case of non-rotating particles. The formulation of the optimum lift force used in this study does not differ from the one applied by Wang et al. (1997) in their numerical simulation of particle-laden channel flow using LES. The optimum lift force is a bundle of different expressions derived generally in simple flow. The regions of applicability of these different expressions are specified by the Stokes and Saffman length scales

$$L_s = \frac{v}{|V_{r,1}|} \quad \text{and} \quad L_G = \sqrt{\frac{v}{|G|}} \tag{6}$$

and also by two dimensionless parameters

$$l^+ = \frac{l}{L_G} \quad \text{and} \quad \epsilon = \text{sign}(GV_{r,1})\frac{Re_G^{1/2}}{Re_s}, \tag{7}$$

where $V_{r,1} = v_1 - u_1^p$ is the instantaneous streamwise velocity difference between the particle and the fluid at the particle location, G is the wall-normal gradient of the instantaneous streamwise fluid velocity at the particle position. The dimensionless parameter ϵ is expressed as a function of two different Reynolds numbers, Re_s and Re_G, the first one is based on $V_{r,1}$ and d_p whereas the second one is based on G and d_p. Therefore, in the case where the particle is located at a distance from the wall lower than L_s and L_G, the dimensional lift force takes the following form Cherukat and McLaughlin (1994):

$$\frac{F_2^L}{\rho_f a_p^2 V_{r,1}^2} = 1.7716 + 0.2160\kappa - 0.7292\kappa^2 + 0.4854\kappa^3 - (3.2397\kappa^{-1} + 1.1450 + 2.0840\kappa - 0.9059\kappa^2)\Lambda + (2.0069 + 1.0575\kappa - 2.4007\kappa^2 + 1.3174\kappa^3)\Lambda^2, \tag{8}$$

where a_p is the particle radius, $\kappa = a_p/l$ and $\Lambda = (a_p G)/V_{r,1}$.

For a particle moving outside this region the dimensional lift force takes the following form:

$$F_2^L = -\frac{9}{\pi}\rho_f a_p^2 V_{r,1}\sqrt{v|G|}\,\text{sign}(G)J \tag{9}$$

where J is a parameter that models the overall contribution of the shear-induced lift and the wall-induced lift. The function J can be divided into two parts so that $J = J_u + J_w$, where J_u and J_w model the shear- and wall-induced lift, respectively. In the present study, these two functions were calculated following the procedure proposed by Wang et al. (1997). Consequently, we will not fully described it hereafter, only a minor difference will be described. This difference concerns the way of computing J_w from the expression proposed by Vasseur and Cox (1977) which is

$$J = -\frac{2\pi^2}{3|\epsilon|}I + J_u, \tag{10}$$

where I is

$$I = \frac{3}{4\pi l^{*2}}\int_0^\infty \int_0^{2\pi} \frac{[\rho^2 + \mathrm{i}l^*\rho\cos(\phi)]^{1/2} + \rho}{[\rho^2 + \mathrm{i}l^*\rho\cos(\phi)]^{1/2} - \rho}\left(\mathrm{e}^{-\rho} - \mathrm{e}^{-[\rho^2+\mathrm{i}l^*\rho\cos(\phi)]^{1/2}}\right)^2 \rho\,\mathrm{d}\rho\,\mathrm{d}\phi, \tag{11}$$

where $l^* = l/L_s$. Vasseur and Cox (1977) evaluated this integral numerically since it has no analytical solution. In order to compute J_w, one could numerically calculate I for each particle at each time step, however in order to get rid of this tedious task, best fit equations were used to approximate the values of I numerically com-

puted by Vasseur and Cox (1977). That method was also preferred by Chen and McLaughlin (1995), but contrary to us they approximated the integral without taking into account the ratio $3/(4\pi l^{*2})$. For the present simulation, we developed best fit equations for I based on 4th order polynomials which are expressed as

$$I = -3.1.10^{-4} l^{*4} + 3.53.10^{-3} l^{*3} - 1.088.10^{-2} l^{*2} - 9.86.10^{-3} l^{*} + 9.57.10^{-2}, \quad (12)$$

when $0 \leqslant l^{*} \leqslant 4.5$,

$$I = 6.78.10^{-7} l^{*4} - 4.81.10^{-5} l^{*3} + 1.26.10^{-3} l^{*2} - 1.485.10^{-2} l^{*} + 7.05.10^{-2}, \quad (13)$$

when $4.5 < l^{*} \leqslant 25$, and

$$I = 0. \quad (14)$$

when $l^{*} \geqslant 25$.

As can be seen from Fig. 1, this way of estimating I yields better agreement, especially for small values of l^{*}, with the numerical results obtained by Vasseur and Cox (1977) in comparison with the method chosen by Chen and McLaughlin (1995). It has to be emphasized that the optimum lift developed by Wang et al. (1997) was derived from previous existing expressions which were developed under various assumptions. Consequently, the optimum lift force can be considered as valid in a steady flow with weak or strong linear shear, and for particles moving at a constant velocity and parallel to the wall. Despite these restrictions, this formulation is more suitable for the simulation of particle-laden wall-bounded flows than the Saffman formula. This is due to the fact that the Saffman formula was designed considering unbounded flows with strong linear shear.

4. Numerical simulation results

4.1. Choice of the particle parameters

The simulations presented here were run for three sets of particles characterized by different Stokes particle response times in wall units, $\tau_p^+ = 1.2$, 6.8 and 27.1, in order to investigate the influence of the optimum lift force and corrected drag force for various particle inertia. The corresponding dimensionless diameters are $d_p/\delta = 0.5 \times 10^{-3}$, 0.7×10^{-3} and 1.4×10^{-3}, for which density ratios, ρ_p/ρ_f, are 2500, 7333 and 7333, respectively. Furthermore, the numerical computations for these three sets of particles were carried out with and without including the optimum lift force and the wall-corrected drag force in the equation of motion. These two different cases will be referred to hereafter as case 1 and case 2, respectively. For the initialization and the computation of the statistics of the dispersed phase, the domain is divided in the wall-normal direction into 128 slices, with the slice thickness being equal to the wall-normal grid spacing. Initially, 5000 solid particles

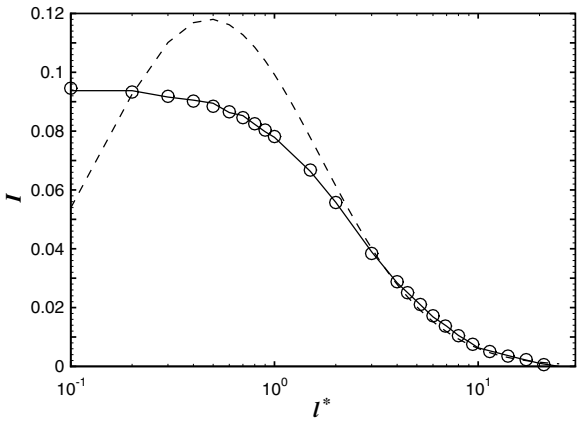

Fig. 1. Numerical results for I as a function of l^{*}. Lines: (—) Vasseur and Cox (1977); (– –) Chen and McLaughlin (1995); (○) Eqs. (12) and (13).

were distributed homogeneously in each slice, and their initial velocity was set equal to the surrounding fluid velocity. The total number of particles was thus 640 000. Statistics on the dispersed phase were started after a time lag of approximately $t^+ = 600$ in order to get results independent of the imposed initial conditions, moreover this time lag is the time necessary for particle statistics (with the exception of the mean concentration) to reach a stationary state. Concerning the smooth wall boundary conditions of the dispersed phase, perfectly elastic collisions were assumed when the particle centre was at a distance from the wall lower than one radius. Furthermore, as soon as particles moved out of the computational domain, they were re-introduced via periodic boundary conditions.

4.2. Balance between the mean drag and lift forces

Before presenting the results, we have to recall that the wall-corrected drag coefficients and the lift force expressions are strictly valid if $Re_p \ll 1$. In order to verify the validity of the latter hypothesis during the simulations, an a posteriori computation of the mean particle Reynolds number $\langle Re_p \rangle = \langle \|\mathbf{V}_r\| \rangle d_p/\nu$ was conducted. The mean magnitude of the relative velocity was approximated from the mean and the variance of the relative velocity by $\langle \|\mathbf{V_r}\| \rangle \approx (\langle V_{r,i} \rangle \langle V_{r,i} \rangle + \langle V'_{r,i} V'_{r,i} \rangle)^{1/2}$. The maximum values of $\langle Re_p \rangle$, calculated from the approximated mean relative velocity magnitude, are 0.03, 0.17 and 0.65 for $\tau_p^+ = 1.2$, $\tau_p^+ = 6.8$ and $\tau_p^+ = 27.1$, respectively. Therefore, even for the largest particles, errors occurring in the estimation of the lift force and drag correction are not expected to significantly affect the dispersed phase statistics presented hereafter.

The average streamwise and wall-normal drag force components acting on particles per unit mass, f_1^D and f_2^D, respectively, are plotted in dimensionless form (with respect to u_τ and δ) in Fig. 2. These forces have been computed as a function of y^+ for $\tau_p^+ = 1.2$, $\tau_p^+ = 6.8$ and $\tau_p^+ = 27.1$ particles, using or not the wall-corrections. From Fig. 2(a), it can be seen that the effects of the correction on the drag coefficient are negligible for the $\tau_p^+ = 1.2$ particles in the streamwise and wall-normal directions. The same behaviour is noticed for $\tau_p^+ = 6.8$. However, for the largest inertia, the mean streamwise drag force per unit mass decreases when the drag corrections are applied except in the region $y^+ > 100$. From our calculations, the mean streamwise relative velocity (not shown here) is also seen to decrease when the corrections are used. Thus a possible explanation is that the solid particles which arrived in the near-wall region encounter low fluid velocity, and if wall corrections are applied, the drag force increases and thus the particles decelerate more rapidly than if no wall-corrections were used. This rapid deceleration induces a diminution in the mean relative velocity and then in the mean streamwise drag force. On the contrary, in the wall-normal direction no significant effect of the use or not of the wall-correction of the drag coefficient is seen. From a qualitative point of view, it can be observed that the drag force per unit mass in the streamwise or in the wall normal directions decreases with increasing particle inertia. The mean drag force per unit mass can also be seen as a part or the whole mean acceleration undergone by the particles, thus this trend just characterized the well-known property of low particle inertia to respond more quickly to the turbulent fluid fluctuations than high particle inertia. In order to quantify the importance of the lift force with respect to the drag force, the ratio of the lift force to the wall-normal component of the drag force is shown in Fig. 3 for $\tau_p^+ = 1.2$, $\tau_p^+ = 6.8$ and $\tau_p^+ = 27.1$. From these results, it is clear that the "optimum" lift force does not represent a significant contribution in the particle motion at the exception of the region $y^+ < 5$ for the largest particles. The lift force exceeds the drag force by 6.5 times, however in this part of the channel the forces acting on the particles are small. Consequently, the lift force would certainly not change considerably the overall behaviour of the particles having the largest inertia. Taking these observations into consideration, the corrections of the drag coefficient as well as the "optimum" lift force are not expected to significantly influence the statistics presented hereafter.

4.3. Particle distribution

An important feature of gas–solid flows is the concentration of particles across the channel width. In Fig. 4 the mean concentration profiles normalized by the bulk concentration are presented. As can be seen, there is no real influence of the corrections of the drag and optimum lift forces on particle concentration profiles except in the region very close to the wall for highest particle inertia. A log–log scale is used in order to better

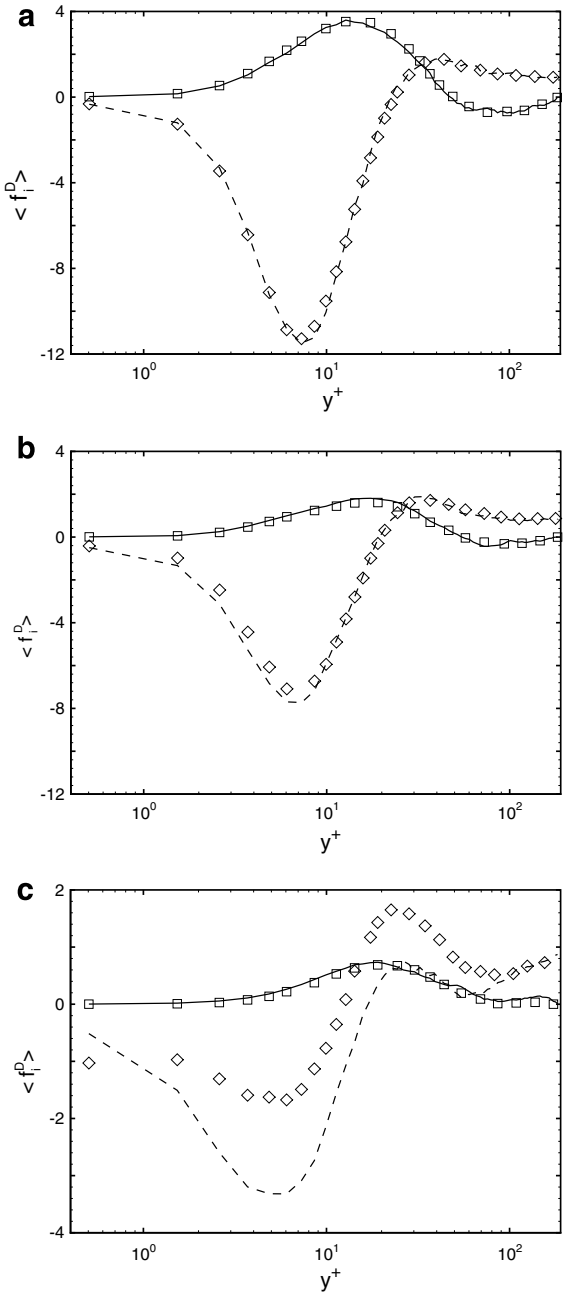

Fig. 2. Mean streamwise and wall-normal drag forces per unit mass. (a) $\tau_p^+ = 1.2$, (b) $\tau_p^+ = 6.8$ and (c) $\tau_p^+ = 27.1$. Symbols (case 1): (◇) f_1^D; (□) f_2^D. Lines (case 2): (– –) f_1^D; (—) f_2^D.

distinguish the concentration in the vicinity of the wall and to better differentiate the profiles for each relaxation time, however one has to be aware that the differences are diminished. At the wall, the near-wall corrections induce a decrease of about 10% in the mean concentration of the $\tau_p^+ = 27.1$ particles. On the contrary, these near-wall corrections make the concentration increase for $1 < y^+ < 4$. As can be seen, as inertia increases the particle concentration increases in the viscous sub-layer and decreases for higher y^+. Note that there is no large difference between the profiles of intermediate and high particle inertia. However, in the near-wall region it is noticed that for larger particle relaxation time, the wall particle concentration exceeds the

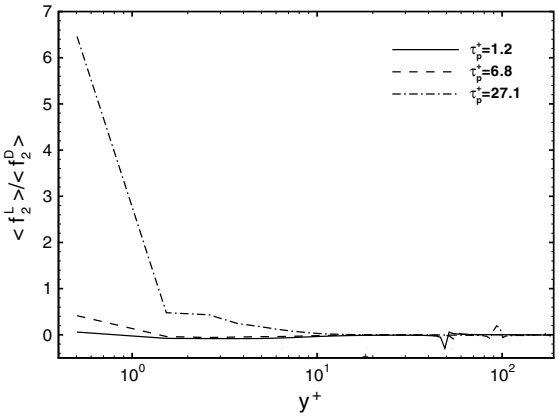

Fig. 3. Ratio of the mean lift force to the mean wall-normal drag force.

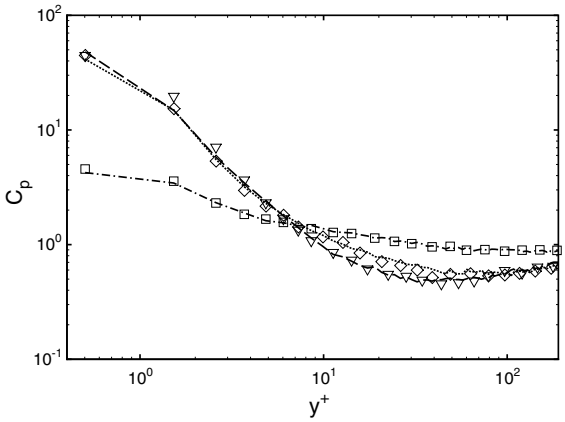

Fig. 4. Mean concentration at time $t^+ = 1210$. Symbols (case 1): (□) $\tau_p^+ = 1.2$; (◇) $\tau_p^+ = 6.8$; (▽) $\tau_p^+ = 27.1$. Lines (case 2): (–·–) $\tau_p^+ = 1.2$; (···) $\tau_p^+ = 6.8$; (– –) $\tau_p^+ = 27.1$.

mean concentration in the channel by 50 times. In such a case, the ''one-way coupling'' hypothesis is obviously not correct. Furthermore, the assumptions of neglecting the influence of particle-particle collisions and real particle-wall collisions appear utterly unjustified, and could be of some importance in the prediction of particle dispersion and deposition phenomena near the wall. Nevertheless, such results, which are consistent with the results reported in the literature (Caporaloni et al., 1975), can be explained by the turbophoresis phenomena which combines the particle inertia effect and the wall-turbulence distribution (Reeks, 1983). From a physical viewpoint, the accumulation of particles in the proximity of the wall can be explained by the presence of typical vortices named ''offspring vortices''. According to Marchioli and Soldati (2002), these vortices seem to be responsible for the particle accumulation under the low-speed streaks which are long-lived wall structures.

4.4. Dispersion results

4.4.1. Fluid and particle mean streamwise and rms velocities

Fig. 5 shows the mean streamwise velocity profile for both particles and fluid as a function of the wall-normal coordinate y^+. Profiles were averaged over a time $t^+ = 800$. As already observed in a channel flow (Picciotto et al., 2004) or in a pipe flow (Portela et al., 2002), the particle inertia effect is seen to be negligible except outside the viscous sublayer, in the region $5 < y^+ < 50$. This particle behaviour can be explained by the trend of particles

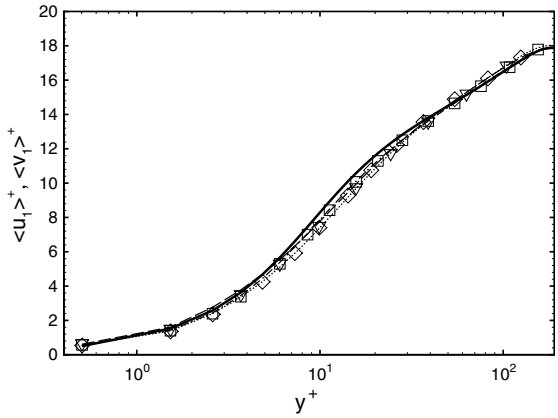

Fig. 5. Mean streamwise fluid and particles velocities. Symbols (case 1): (□) $\tau_p^+ = 1.2$; (◇) $\tau_p^+ = 6.8$; (▽) $\tau_p^+ = 27.1$. Lines (case 2): (—) fluid; (–·–) $\tau_p^+ = 1.2$; (···) $\tau_p^+ = 6.8$; (– –) $\tau_p^+ = 27.1$.

to accumulate in the low speed streaks characterized by a negative streamwise fluid fluctuating velocity at particle's location (see Fig. 8). The mean streamwise particle velocity is seen to not be affected by the use of the correction of the drag and of the optimum lift force in the case of small particle inertia, while the use of these near-wall corrections yields a slight decrease of the mean streamwise velocity for the $\tau_p^+ = 27.1$ particles in the near-wall region. From the particle rms velocity profiles (Fig. 6), a similar conclusion can be drawn in the streamwise direction. However, in the wall-normal and spanwise directions, the rms velocities are not significantly affected by the wall-corrections even in the vicinity of the wall. Similarly the force corrections do not affect the results on the off-diagonal component (see Fig. 7).

4.4.2. Drift velocities

Fig. 8 shows the drift velocity $\langle u_1^{fp} \rangle$ profiles as a function of the wall-normal coordinate y^+. No real influence of the corrections of the forces are clearly noticed. The use of the optimum lift force and corrections of the drag coefficient seems therefore to have a negligible impact on particle statistics such as the drift and particle velocities.

Physical considerations can be emphasized from the values of the mean drift velocities (in the streamwise and wall-normal directions). Negative values of the mean streamwise drift velocity are observed whereas positive values of the wall-normal drift velocities appear for $y^+ < 45$ and this trend is inverted for $y^+ > 45$. However, the cross-over point is not the same in the streamwise or wall-normal directions. The value of the cross-over point is the same as obtained by Picciotto et al. (2004) in the wall-normal direction, the curves cross over at $y^+ \approx 45$ whatever the inertia. In the streamwise direction, the curves cross over at $y^+ \approx 25$ whatever the inertia. Such negative values of the mean streamwise drift velocity are physically associated with the preferential concentration phenomenon. Particles accumulate in streamwise oriented streaks correlated with the so-called low speed streaks in wall turbulence, characterized by negative values of the mean streamwise drift velocity. At the same time, positive values of the wall-normal drift velocity are noticed (see Fig. 8) for higher particle inertia, meaning that particles sample preferentially ejection-like environment as previously observed (Picciotto et al., 2004). The wall-normal drift velocity becomes negative outside the near-wall region reaching a local maximum at $y^+ \approx 75$. Sweep and ejection events seem to be to responsible for the particle distribution in the channel. By referring to the quadrant analysis (Wallas et al., 1972) particle transfer fluxes can be elucidated as done by Marchioli and Soldati (2002). The product between instantaneous streamwise and wall-normal drift velocities can be considered as an instantaneous realization of the Reynolds stresses, and the sign of such a product reveals four types of events. The events which are of particular interest are the ones which correspond to a negative value of the instantaneous streamwise drift velocity associated with a positive value of wall-normal one (so-called Q_2 type event) and the second one is related to positive values of the instantaneous streamwise drift velocity and negative values of the instantaneous wall-normal velocity

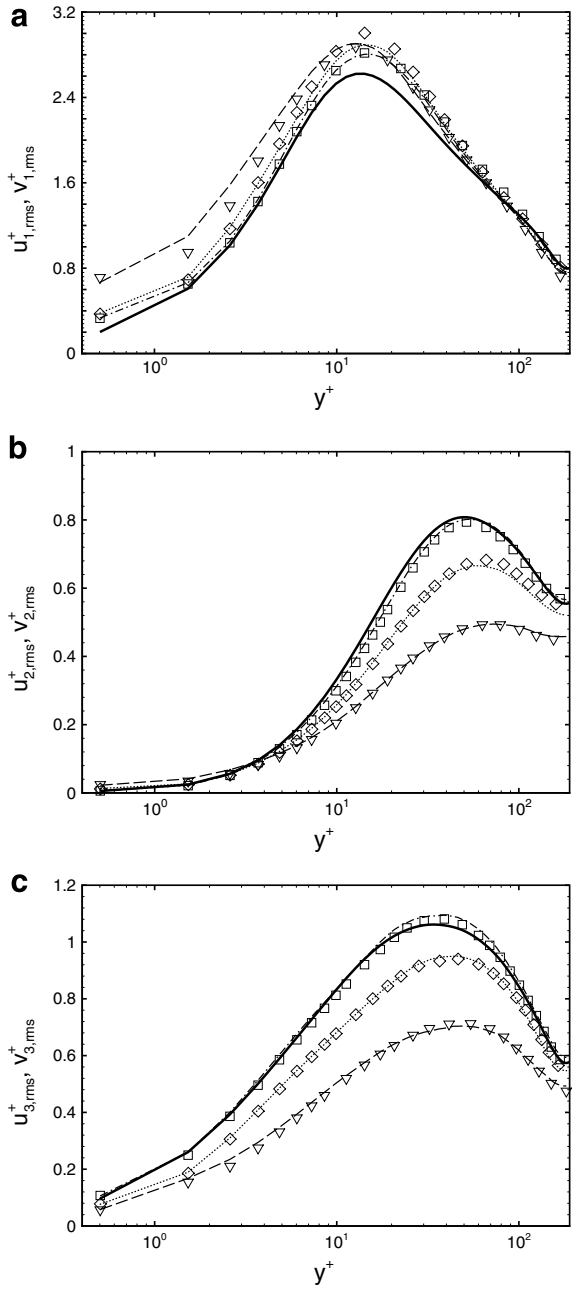

Fig. 6. Root mean square of the fluid and particle velocities. (a) Streamwise, (b) wall-normal and (c) spanwise. Symbols and lines: same as in Fig. 5.

(so-called Q_4 type event). The Q_2 type event characterizes the particle transfer from the wall region to the outer flow (ejection) in opposite to the sweeps events which drive particles to the wall corresponding to the Q_4 type event. The scenario proposed by Marchioli and Soldati (2002) where sweeps and ejections events play a role on particles transfer via the quadrant analysis seems to be valid according to the results obtained in the present study. We have also tested the influence of the force's corrections on the fluid Reynolds tensor at the solid particle location (results not shown here) and the same conclusion was drawn: the results are not sensitive to the near-wall force corrections.

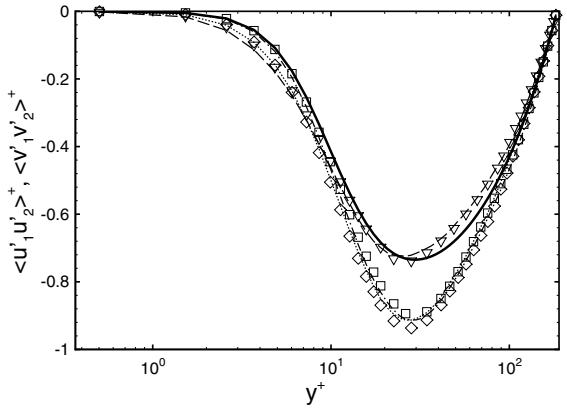

Fig. 7. Fluid and particle shear stress. Symbols and lines: same as in Fig. 5.

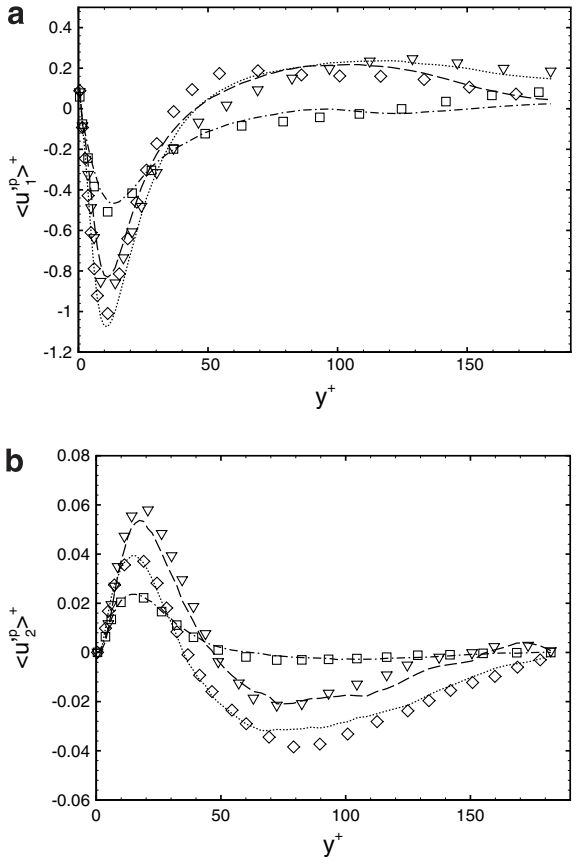

Fig. 8. Drift velocities. (a) Streamwise. (b) Wall-normal. Symbols and lines: same as in Fig. 4.

4.4.3. Fluid-particle covariances

Figs. 9 and 10 show the diagonal and off-diagonal components of the fluid-particle covariance tensor, respectively, as a function of the wall-normal coordinate y^+. No real influence of the corrections of the forces on such statistics is clearly observed. A little decrease is obtained for the intermediate inertia in the streamwise

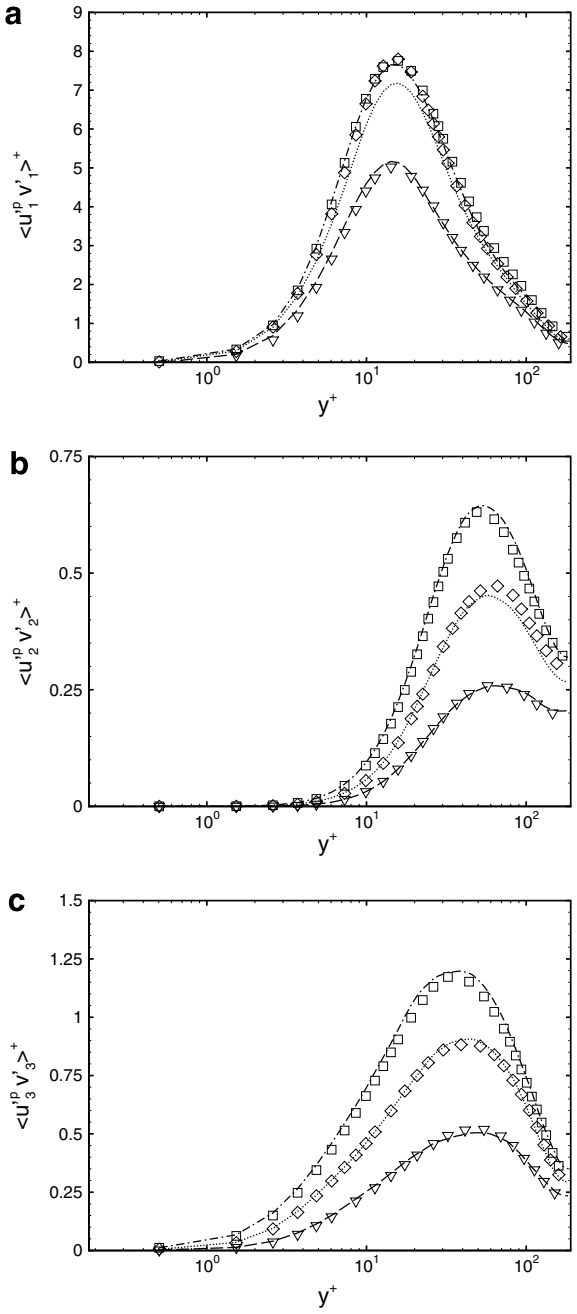

Fig. 9. Diagonal components of the covariance fluid-particle tensor. Symbols and lines: same as in Fig. 4.

direction. The present results are conform to the literature since the diagonal components are found to decrease with particle inertia whatever the directions as previously observed by Wang and Squires (1996a). They used a two-phase flow LES simulation in which various τ_p^+ ranging from 9 up to 800 were tested. A qualitative comparison with the results obtained for the lower value of τ_p^+ can be made. In that sense, as Wang and Squires (1996a), the streamwise covariance is found to be the largest comparing with the others diagonal components. Concerning the off-diagonal component, a little asymmetry of the curves is observed which would be more apparent when particle inertia increases according to the results of Wang and Squires (1996a).

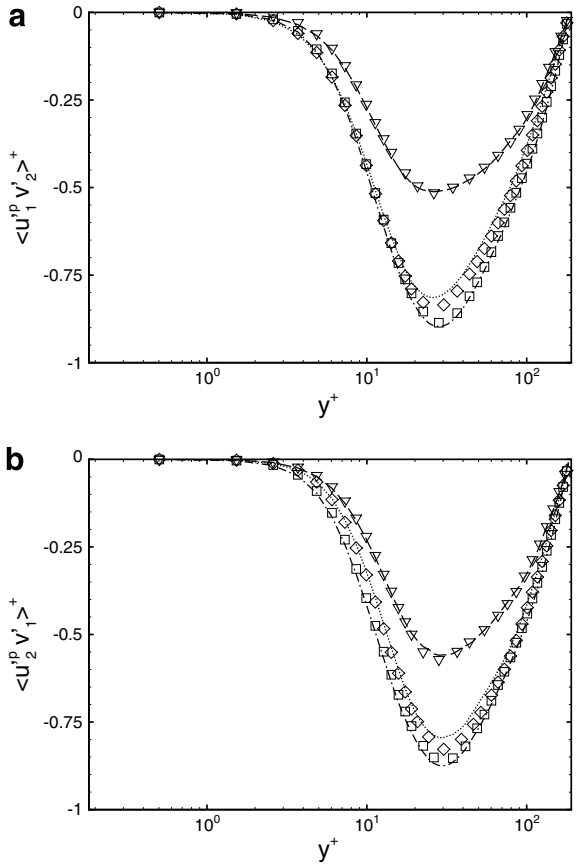

Fig. 10. Off-diagonal components of the covariance fluid-particle tensor. Symbols and lines: same as in Fig. 4.

5. Conclusion

The influence of the wall-corrections of the drag coefficient and of the lift force on the dispersed phase statistics has been investigated in the case of moderate Reynolds number gas–solid channel flow simulation without external forces. Results show that the drag corrections and the use of the optimum lift force have a negligible impact on the dispersed phase statistics such as concentration profiles, mean streamwise fluid and particles velocities, root mean square of the particle velocities, drift velocities, fluid Reynolds tensor at particle location and fluid-particle covariance tensor. Consequently, the main phenomena (dispersion and deposition) involved in particle-laden channel flows are not expected to be strongly affected by these quite small differences. These results are consistent with the LES study by Wang et al. (1997), which was devoted to the influence of the lift force in the simulations of particle deposition in confined turbulent flows, since they found a small overall effect of this force on the deposition rates. Taking these results into consideration, we believe that the introduction, in the particle equation of motion, of the quite complicated formulation of the optimum lift force and the corrections of the drag force is not necessary. This conclusion is only valid under certain restrictions such as the absence of gravity force and purely elastic particle-wall collisions, since these two latter effects could largely increase the mean streamwise relative velocity and thus the lift force.

References

Benson, M., Tanaka, T., Eaton, J., 2005. Effects of wall roughness on particle velocities in a turbulent channel flow. J. Fluids Eng. 127, 250–256.

Brenner, H., 1961. The slow motion of a sphere through a viscous fluid towards a plane surface. Chem. Eng. Sci. 16, 242–251.

Caporaloni, M., Tampeiri, F., Trombetti, F., Vittori, O., 1975. Transfer of particles in nonisotropic air turbulence. J. Atmos. Sci. 32, 565–568.

Chen, M., McLaughlin, J., 1995. A new correlation for the aerosol deposition rate in vertical ducts. J. Colloid Interf. Sci. 169, 437–455.

Cherukat, P., McLaughlin, J., 1994. The inertial lift on a rigid sphere in a linear shear flow field near a flat wall. J. Fluid Mech. 263, 1–18.

Faxen, H., 1923. Die bewegung einer starren kugel längs der achse eines mit zährer flüssigkeit gefüllten rohres. Arkiv Mat. Astron. Fys. 17, 1–28.

Fukagata, K., Zahrai, S., Bark, F.H., Kondo, S., 1999. Influences of the near-wall drag correction in a lagrangian simulation of particulate turbulent channel flow. In: Proceedings of the First Symposium on Turbulence and Shear Flow Phenomena. Vol. 6. Begell House, New York, pp. 259–264.

Kulick, J., Fessler, J., Eaton, J., 1994. Particle response and turbulence modification in fully developed channel flow. J. Fluid Mech. 277, 109–134.

Marchioli, C., Soldati, A., 2002. Mechanisms for particle transfer and segregation in a turbulent boundary layer. J. Fluid Mech. 468, 283–315.

Maude, A., 1963. The movement of a sphere in front of a plane at low reynolds number. Brit. J. Appl. Phys. 14, 894–898.

Morsi, S., Alexander, A., 1972. An investigation of particle trajectories in two-phase flow systems. J. Fluid Mech. 55, 193–208.

Orlandi, P., 2000. Fluid Flow Phenomena. A numerical toolkit. Kluwer Academic Publishers.

Picciotto, M., Marchioli, C., Reeks, M., Soldati, A., 2004. On the preferential concentration of inertial particles dispersed in a turbulent boundary layer. In: Proceedings of third International Symposium on Two-phase flow modelling and Experimentation. Pisa, Italy.

Portela, L., Cota, P., Oliemans, R., 2002. Numerical study of the near-wall behavior of particles in turbulent pipe flows. Pow. Tec. 125, 149–157.

Reeks, M.W., 1983. The transport of discrete particles in inhomogeneous turbulence. J. Aerosol Sci. 14, 729–739.

Rizk, M., Elghobashi, S., 1985. The motion of a spherical particle suspended in a turbulent flow near the wall. Phys. Fluids 28, 806–817.

Rovelstad, A., Handler, R., Bernard, S., 1994. The effect of interpolation errors on the lagrangian analysis of simulated turbulent channel flow. J. Comput. Phys. 110, 190–195.

Vasseur, P., Cox, R., 1977. The lateral migration of a spherical particle sedimenting in a stagnant bounded fluid. J. Fluid Mech. 78, 561–591.

Wakiya, S., 1960. Research report 9. Faculty of Engineering, Niigata University, Japan.

Wallas, J.M., Eckelmann, H., Brodkey, R.S., 1972. The wall region in turbulent shear flow. J. Fluid Mech. 54, 39–48.

Wang, Q., Squires, K., 1996a. Large eddy simulation of particle deposition in a vertical turbulent channel flow. Int. J. Multiphase Flow 22, 667–683.

Wang, Q., Squires, K., 1996b. Large eddy simulation of particle-laden turbulent channel flows. Phys. Fluids 8, 1207–1223.

Wang, Q., Squires, K., Chen, M., McLaughlin, J., 1997. On the role of lift force in turbulence simulations of particle deposition. Int. J. Multiphase Flow 23, 749–763.